White Matter Connectivity Abnormalities in Prediabetes and Type 2 Diabetes: The Maastricht Study

Diabetes Care 2020;43:201–208 | https://doi.org/10.2337/dc19-0762

Laura W. Vergoossen,[1,2,3]
Miranda T. Schram,[3,4,5] Joost J. de Jong,[1,2]
Coen D. Stehouwer,[3,4]
Nicolaas C. Schaper,[3,4,6]
Ronald M. Henry,[3,4,5]
Carla J. van der Kallen,[3,4]
Pieter C. Dagnelie,[3,4] Martin P. van Boxtel,[2]
Simone J. Eussen,[3,7] Walter H. Backes,[1,2]
and Jacobus F. Jansen[1,2,8]

OBJECTIVE

Prediabetes and type 2 diabetes are associated with structural brain abnormalities, often observed in cognitive disorders. Besides visible lesions, (pre)diabetes might also be associated with alterations of the intrinsic organization of the white matter. In this population-based cohort study, the association of prediabetes and type 2 diabetes with white matter network organization was assessed.

RESEARCH DESIGN AND METHODS

In the Maastricht Study, a type 2 diabetes–enriched population-based cohort study (1,361 subjects with normal glucose metabolism, 348 with prediabetes, and 510 with type 2 diabetes assessed by oral glucose tolerance test; 52% men; aged 59 ± 8 years), 3 Tesla structural and diffusion MRI was performed. Whole-brain white matter tractography was used to assess the number of connections (node degree) between 94 brain regions and the topology (graph measures). Multivariable linear regression analyses were used to investigate the associations of glucose metabolism status with network measures. Associations were adjusted for age, sex, education, and cardiovascular risk factors.

RESULTS

Prediabetes and type 2 diabetes were associated with lower node degree after full adjustment (standardized [st]$\beta_{Prediabetes}$ = −0.055 [95% CI −0.172, 0.062], st$\beta_{Type2diabetes}$ = −0.256 [−0.379, −0.133], P_{trend} < 0.001). Prediabetes was associated with lower local efficiency (stβ = −0.084 [95% CI −0.159, −0.008], P = 0.033) and lower clustering coefficient (stβ = −0.097 [95% CI −0.189, −0.005], P = 0.049), whereas type 2 diabetes was not. Type 2 diabetes was associated with higher communicability (stβ = 0.148 [95% CI 0.042, 0.253], P = 0.008).

CONCLUSIONS

These findings indicate that prediabetes and type 2 diabetes are associated with fewer white matter connections and weaker organization of white matter networks. Type 2 diabetes was associated with higher communicability, which was not yet observed in prediabetes and may reflect the use of alternative white matter connections.

[1]Department of Radiology and Nuclear Medicine, Maastricht University Medical Center+ (MUMC+), Maastricht, the Netherlands
[2]School for Mental Health and Neuroscience (MHeNs), Maastricht University, Maastricht, the Netherlands
[3]School for Cardiovascular Disease (CARIM), Maastricht University, Maastricht, the Netherlands
[4]Department of Internal Medicine, Maastricht University Medical Center+, Maastricht, the Netherlands
[5]Heart and Vascular Centre, Maastricht University Medical Center+, Maastricht, the Netherlands
[6]School for Public Health and Primary Care (CAPHRI), Maastricht University, Maastricht, the Netherlands
[7]Department of Epidemiology, Maastricht University, Maastricht, the Netherlands
[8]Department of Electrical Engineering, Eindhoven University of Technology, Eindhoven, the Netherlands

Corresponding author: Jacobus F. Jansen, jacobus.jansen@mumc.nl

Type 2 diabetes is associated with cognitive decline (1–3) and poses an increased risk for brain diseases, such as Alzheimer disease and depression (4,5). As type 2 diabetes is associated with abundant macro- and microvascular disease, it may also affect brain vessels, leading to cerebral small vessel disease (e.g., white matter lesions [WMLs]) and neurodegeneration (brain atrophy) (6,7), which represent early features in the pathophysiology of cognitive decline and dementia (8) and can be measured by brain MRI. Some studies even show that prediabetes is already associated with alterations in the brain (9,10), more specifically with the presence of lacunar infarcts, larger WML volumes, and smaller white matter volumes, with further deterioration in type 2 diabetes, as previously reported (7). The white matter is organized as a complex network of connected fibers, which is responsible for efficient information exchange between brain regions. Alterations in one region may affect the function of other regions to which they are connected via white matter tracts. Thus, to understand the organization of white matter networks entirely, the assessment of regional brain volumes is insufficient. The use of diffusion MRI–derived white matter tracts, in combination with graph theoretical analysis, does address both the regional volumes and its connections to other regions.

Type 2 diabetes might also be associated with alterations in the intrinsic organization of the white matter (11–14). However, whether changes in the intrinsic network organization of the white matter already occur in prediabetes is currently unknown (15–17). We hypothesize that brain abnormalities comparable to those found in type 2 diabetes are, to a lesser extent, already present in prediabetes, possibly already before the onset of cognitive decline. The main objective of this study is to assess the association of prediabetes and type 2 diabetes with white matter network characteristics in terms of the number (node degree) and organization (graph measures) of the white matter connections.

RESEARCH DESIGN AND METHODS

The Maastricht Study: Population and Design

We used data from the Maastricht Study, an observational, prospective, population-based cohort study. The rationale and methodology have been described previously (18). In brief, the study focuses on the etiology, pathophysiology, complications, and comorbidities of type 2 diabetes and is characterized by an extensive phenotyping approach. Eligible for participation were all individuals aged between 40 and 75 years and living in the southern part of the Netherlands. Participants were recruited through mass media campaigns and from the municipal registries and the regional Diabetes Patient Registry via mailings. Recruitment was stratified according to known type 2 diabetes status, with an oversampling of individuals with type 2 diabetes, for reasons of efficiency. Participants with type 1 diabetes or other types of diabetes were excluded from the analysis. The present report includes cross-sectional data from the first 3,451 participants, who completed the baseline survey between November 2010 and September 2013. The examinations of each participant were performed within a time window of 3 months. MRI measurements were implemented from December 2013 onwards until February 2017 and were available in 2,318 out of 3,451 participants. Of the 2,318 participants with MRI measurements available, 2,302 subjects had complete data without artifacts (flowchart in Supplementary Fig. 1). The study has been approved by the institutional medical ethical committee (NL31329.068.10) and the Dutch Ministry of Health, Welfare, and Sports of the Netherlands (permit 131088-105234-PG). All participants gave written informed consent.

Glucose Metabolism Status

To determine glucose metabolism status, all participants, except those who used insulin, underwent a standardized 2-h 75-g oral glucose tolerance test (OGTT) after an overnight fast. For safety reasons, participants with a fasting blood glucose (FBG) level >11.0 mmol/L, as determined by a finger prick, did not undergo the OGTT. For these individuals, fasting glucose level and information about diabetes medication were used to determine glucose metabolism status. Glucose metabolism status was defined according to the World Health Organization 2006 criteria into normal glucose metabolism (NGM), prediabetes, and type 2 diabetes (19). Participants were considered to have type 2 diabetes if they had an FBG ≥7.0 mmol/L or a 2-h postload blood glucose ≥11.1 mmol/L or used oral glucose-lowering medication or insulin. They were considered to have prediabetes if they had an FBG ≥6.1 mmol/L and/or a 2-h postload blood glucose ≥7.8 mmol/L, and NGM if they had an FBG <6.1 mmol/L and a 2-h postload blood glucose <7.8 mmol/L and no use of diabetes medication.

MRI

MRI was performed on a 3 Tesla MRI scanner (MAGNETOM Prisma-fit Syngo MR D13D; Siemens Healthcare, Erlangen, Germany) using a 64-element head/neck coil for parallel imaging with an acceleration factor of two. A 3D T1–weighted magnetization prepared rapid acquisition gradient echo (MPRAGE) sequence (TR/TI/TE 2,300/900/2.98 ms, 176 slices, 256 × 240 matrix size, and 1.00 mm cubic voxel size) was acquired for anatomic reference. Diffusion-weighted MRI (dMRI) data were acquired using a diffusion-sensitized echo-planar imaging (EPI) sequence (TR/TE 6,100/57 ms, 65 slices, 100 × 100 matrix size, 2.00 mm cubic voxel size, and 64 diffusion-sensitizing gradient directions [b = 1,200 s/mm^2]). In addition, three minimally diffusion-weighted images (b = 0 s/mm^2) were acquired.

Image Preprocessing

To define n = 94 regions, the automatic anatomical labeling 2 (AAL2) atlas (20) was used. The AAL2 volumes of interest were transformed to diffusion space for each individual subject. First, affine registrations of the dMRI image to the T1 image and of the T1 image to T1 MNI-152 standard space (21) were performed. These two transformations were combined, and the inverse transformation matrix was applied to the AAL2 template. T1-weighted and fluid-attenuated inversion recovery (FLAIR) images were segmented by use of an ISO13485:2012-certified, automated method (which included visual inspection) (22,23) into white matter, gray matter, cerebrospinal fluid, and WML. Detailed methods were previously described (7). dMRI data analysis was performed with the diffusion MR Toolbox ExploreDTI version 4.8.6 (24). The main preprocessing steps were eddy current–induced geometric distortions and head motion correction, and

estimation of the diffusion tensor. After preprocessing, fiber orientation distributions (FODs) were estimated using constrained spherical deconvolution with a maximum harmonic degree of 8 (25), which allows fiber tracking through regions with crossing fibers. Whole-brain deterministic tractography was performed using FOD sampling (26) with a seed point resolution of 2 mm^3, a step size of 1 mm, and an FOD and maximum deflection angle threshold of 0.1 and 30°, respectively. The next step was performing connectivity analysis to obtain white matter tracts from and to all the segmented regions. A previous study of our group confirmed the robustness of tract volume as a measure for the edge weighting (27). Therefore, for each connection, the tract volume was calculated as the number of voxels visited by at least one tract between concerned areas multiplied by the voxel volume (in mm^3). The obtained connectivity matrix with tract volumes was normalized to intracranial volume to reduce intersubject variation (28). When regions were connected by only one or two streamlines, the corresponding tract volumes were removed from the connectivity matrix, as an additional noise filter.

White Matter Networks

Network analysis was performed using the Brain Connectivity Toolbox (version 2017-15-01) (29) in MATLAB (Release 2016a; The MathWorks, Inc., Natick, MA). In this method (for an overview, see Fig. 1), the brain is represented as a graph, which is a network of nodes (i.e., gray matter brain regions) connected by edges (i.e., white matter connections between brain regions). The organization of such a graph can be characterized by the use of graph measures, e.g., clustering coefficient, local efficiency, communicability, and global efficiency. These graph measures describe the efficiency and integrity of the white matter networks.

The node degree is calculated for each AAL2 region, and the mean value is defined as the average node degree, which is a measure for the average number of edges connected to a region (node). In a network with a high average node degree, nodes are connected to many other nodes in the network (i.e., strong innervation). The sparsity of a network is the ratio of the number of missing connections in a network to the possible number of connections and is closely, but inversely, related to the node degree. The sparsity ranges from 0 to 1; the higher the sparsity, the lower the density of the network (29).

Graph Measures

To describe network organization, measures indicative of network segregation were calculated to assess the presence of local densely interconnected groups of brain regions, and measures indicative of integration were calculated to assess large-scale communication between nodes (see Fig. 1). Measures of segregation describe the local connectivity properties of a network and comprise clustering and local efficiency. The clustering coefficient quantifies the number of connections between the nearest neighbors of a region as a proportion of the maximum number of possible connections (15). The local efficiency of a region is the inverse of the average shortest path connecting all neighbors of that region (30). Paths are sequences of connections in the network, which represent potential routes for communication between brain regions.

Measures of integration describe the ease with which brain regions communicate in terms of paths and include global efficiency and communicability. The global efficiency is the inverse of the average shortest path length calculated over the entire brain; thus, a high global efficiency reflects long paths between regions (30). However, neural communication does not necessarily follow the shortest paths only; slightly longer paths might also be used (e.g., to bypass affected paths). Therefore, an alternative measure of communication, the communicability, was calculated, which includes all possible paths between brain regions, weighted according to their length (31).

White Matter Structural Connectivity

The node degree was first calculated for the full connectivity matrices of the groups (NGM, prediabetes, and type 2 diabetes) for comparison of the basic
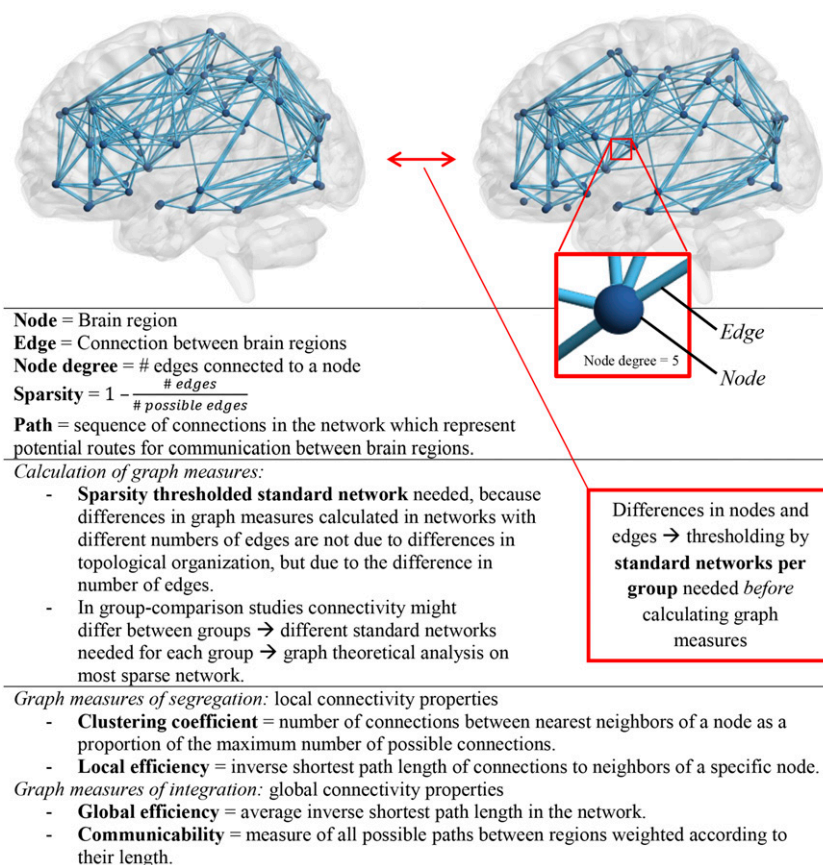

Node = Brain region
Edge = Connection between brain regions
Node degree = # edges connected to a node
Sparsity = $1 - \frac{\# \, edges}{\# \, possible \, edges}$
Path = sequence of connections in the network which represent potential routes for communication between brain regions.

Calculation of graph measures:
- **Sparsity thresholded standard network** needed, because differences in graph measures calculated in networks with different numbers of edges are not due to differences in topological organization, but due to the difference in number of edges.
- In group-comparison studies connectivity might differ between groups → different standard networks needed for each group → graph theoretical analysis on most sparse network.

Differences in nodes and edges → thresholding by **standard networks per group** needed *before* calculating graph measures

Graph measures of segregation: local connectivity properties
- **Clustering coefficient** = number of connections between nearest neighbors of a node as a proportion of the maximum number of possible connections.
- **Local efficiency** = inverse shortest path length of connections to neighbors of a specific node.

Graph measures of integration: global connectivity properties
- **Global efficiency** = average inverse shortest path length in the network.
- **Communicability** = measure of all possible paths between regions weighted according to their length.

Figure 1—Glossary.

network architecture between them. Subsequently, a standard group averaged network was calculated for each group separately (32). Note that these standard networks may differ per group comparison. This standard network was proportionally thresholded to a sparsity of 0.80 (only the connections that were present in at least 80% of the participants in that group will be taken into account in the individual connectivity matrices), resulting in a weighted, undirected network with a sparsity close to the sparsity of the standard network. The standard networks were also thresholded for a range of sparsity values (0.65–0.9, step size 0.05) to assess the robustness over different sparsity values. Additionally, connections were identified with a significantly increased or decreased tract volume. First, we applied thresholding by a network based on only the NGM subjects, to check whether differences in basic network architecture were also present after the exclusion of connections formed due to noise as opposed to pathology. As the networks of the group with type 2 diabetes appeared to be most sparse, subsequently, the organization of this remaining (sub)network was analyzed. Hence, the resulting network contains only the connections of the sparser type 2 diabetes network of which the connections are also present in the other two groups. Otherwise, the "true sparsity" of the subjects with type 2 diabetes would be lower than for the subjects with NGM and prediabetes, which again leads to different results in graph measures due to differences in sparsity. To investigate whether prediabetes is already associated with a structural reorganization, for the comparison of prediabetes and NGM, the average prediabetes-derived network was applied.

To investigate the structural organization in the white matter networks in type 2 diabetes and prediabetes, graph measures of segregation (i.e., clustering coefficient and local efficiency) and integration (i.e., global efficiency and communicability) (15–17) were calculated from the brain graphs. Graph measures were normalized to comparable values from randomly generated networks of equal size and similar connectivity distribution ($n = 100$) (33) and calculated over a range of six sparsity values, 0.65–0.9 (step size 0.05).

General Characteristics and Covariates

Educational level (low, intermediate, and high), smoking status (never, current, and former), and history of cardiovascular disease were assessed by questionnaires (18). Medication use was assessed in a medication interview where generic name, dose, and frequency were registered. We measured weight, height, BMI, waist circumference, blood pressure (measured in office [705IT; Omron, Kyoto, Japan]), and plasma lipid profile (18).

Statistical Analysis

All statistical analyses were performed using SPSS (SPSS Statistics 23.0; IBM, Chicago, IL). Clinical characteristics of the participants within the three groups of glucose metabolism status were compared using ANOVA and Pearson χ^2 tests, where appropriate. Multivariable linear regression was used to investigate the association of glucose metabolism status with average node degree and graph measures. For linear trend analyses, the categorical variable glucose metabolism status (NGM = 0, prediabetes = 1, and type 2 diabetes = 2) was used in the regression models. To assess regression coefficients per glucose metabolism group, analysis with dummy variables for prediabetes and type 2 diabetes, with NGM as the reference group, was used. Analyses were adjusted for potential confounders, notably age, sex, education level, and MRI date (model 1), and additionally adjusted for cardiovascular disease risk factors: BMI, ratio of total cholesterol to HDL, lipid-modifying medication, office systolic blood pressure, antihypertensive medication, and prior cardiovascular disease (model 2). Regression coefficients for normal aging (i.e., in participants with normal compared with abnormal glucose metabolism) were determined in the group with NGM. Multiple linear regression with false discovery rate correction (q value = 0.05) was used to correct for multiple comparisons to determine which connections had significantly different tract volumes between groups, and were adjusted for age, sex, education level, and MRI lag time. In the type 2 diabetes–based standard networks, the associations of glucose metabolism groups and continuous measures of blood glucose with graph measures were analyzed by use of multiple

regression analyses. Analyses on graph measures were adjusted for age, sex, education level, MRI date, and average node degree (model 1), and additionally for cardiovascular disease risk factors (model 2). Furthermore, we investigated the association of hemoglobin A_{1c} (HbA$_{1c}$), FBG, and 2-h postload glucose levels with average node degree and graph measures, and adjusted in an additional model for lifestyle factors. Skewed variables (WML volumes) were log10 transformed. P values <0.05 were considered statistically significant.

RESULTS

General Characteristics of the Study Population

Table 1 shows the general characteristics of the study population for subjects with NGM, prediabetes, and type 2 diabetes. The study population consisted of 2,219 individuals; 1,361 had NGM, 348 had prediabetes, and 510 had type 2 diabetes. Mean age was 59 ± 8 years, and 48% were women. Individuals with prediabetes and type 2 diabetes were older, less often female, more often had an adverse cardiovascular risk profile, and more often had a low educational level (Table 1). Individuals who underwent MRI were younger, less likely to have type 2 diabetes, less often current smokers, and less often had a low education level compared with those who did not undergo MRI (Supplementary Table 1).

Structural Network Characteristics

After full adjustment, the average node degree for the full connectivity matrices (i.e., before thresholding) was significantly lower for subjects with type 2 diabetes compared with NGM (1.3% lower, standardized [st]β = −0.111 [95% −0.220, −0.002], P_{trend} = 0.047) (Supplementary Table 2). Subsequent analysis using the standard network based on only subjects with NGM showed significantly different results for type 2 diabetes compared with prediabetes (0.7% lower, stβ = −0.256 [95% CI −0.379, −0.133], P_{trend} < 0.001). Higher HbA$_{1c}$, FBG, and 2-h postload glucose levels were also associated with lower node degree in the unthresholded and NGM-based networks (Supplementary Table 3).

In Fig. 2A, the standard network for the group with NGM is schematically

Table 1—Clinical characteristics of participants according to glucose metabolism status

Characteristic	NGM (n = 1,361)	Prediabetes (n = 348)	Type 2 diabetes (n = 510)	P_{trend}
Demographics				
Age (years)	57.6 ± 8.1	61.2 ± 7.5	62.5 ± 7.6	<0.001
Sex, male (%)	44.2	55.2	68.6	<0.001
Education level (%), low/middle/high	25.4/28.1/46.4	33.0/31.0/36.0	41.3/30.2/28.5	<0.001
Glucose metabolism				
FBG (mmol/L)	5.2 ± 0.4	5.9 ± 0.6	7.8 ± 1.9	<0.001
2-h postload glucose (mmol/L)*	5.4 ± 1.1	8.1 ± 1.8	14.2 ± 4.1	<0.001
HbA$_{1c}$ (%)	5.4 ± 0.3	5.7 ± 0.4	6.9 ± 1.0	<0.001
HbA$_{1c}$ (mmol/mol)	36.0 ± 3.7	38.6 ± 4.4	51.4 ± 11.0	<0.001
Diabetes duration (years)†	—	—	6.9 ± 7.2	—
Cardiovascular risk factors				
BMI (kg/m^2)	25.5 ± 3.5	27.3 ± 4.0	29.3 ± 4.6	<0.001
Waist circumference (cm)	90.2 ± 10.9	96.8 ± 11.3	104.3 ± 12.9	<0.001
Office systolic blood pressure (mmHg)	131 ± 17	136 ± 16	141 ± 17	<0.001
Office diastolic blood pressure (mmHg)	75 ± 10	78 ± 10	77 ± 9	<0.001
Hypertension, yes (%)	39.1	59.4	82.0	<0.001
Ratio of total cholesterol to HDL	3.6 ± 1.2	3.9 ± 1.2	3.6 ± 1.1	0.152
History of cardiovascular disease, yes (%)	8.9	11.3	21.3	<0.001
History of CVA, yes (%)‡	1.1	2.3	3.9	<0.001
Medication use				
Insulin use, yes (%)†	—	—	19.6	—
Antihypertensive medication, yes (%)	20.6	38.8	70.2	<0.001
Lipid-modifying medication, yes (%)	14.8	29.0	72.5	<0.001
Lifestyle factors				
Alcohol consumption (%), none/low/high	13.9/57.5/28.6	16.3/53.5/30.2	26.4/53.1/20.5	<0.001
Smoking status (%), never/former/current	40.9/47.9/11.1	30.4/58.0/11.6	32.7/53.7/13.5	0.001
Cognitive score				
MMSE total score§	29.2 ± 1.1	28.9 ± 1.1	28.7 ± 1.3	<0.001

Data are presented as means ± SD or percentage and stratified for glucose metabolism status: NGM, prediabetes, and type 2 diabetes. P values indicate trend analysis over glucose metabolism status. CVA, cerebrovascular accident; MMSE, Mini-Mental State Examination. *2-h postload glucose values were available in n = 2,098. †Available in 344 individuals with type 2 diabetes. ‡History of CVA data were available in n = 2,191. §Five participants had an MMSE score of 22 or 23 (mild cognitive impairment) and none had dementia. Detailed protocols of the general measurements are presented in the Supplementary Data. Characteristics of variables used in the additional models (Supplementary Tables 6–11) are given in Supplementary Table 12.

shown. Figure 2*B* and *C* indicate for which connections the tract volumes were significantly different in prediabetes compared with NGM, and in type 2 diabetes compared with NGM, respectively. These results indicate that in prediabetes, only intrahemispheric connections had significantly smaller tract volumes. In type 2 diabetes, both inter- and intrahemispheric connections (of which 66% were interhemispheric) had significantly smaller tract volumes, especially between the frontal lobes and between the frontal and temporal lobe.

As an additional analysis, the association between WML volume and node degree was determined over all subjects. After full adjustment, relative WML volume (in % of intracranial volume) was negatively associated with the node degree of the NGM-based standard network (stβ = −0.059 [95% CI −0.101, −0.018], P = 0.001). This association was not present for the smaller type 2 diabetes–based standard network (stβ = −0.010 [95% CI −0.035, 0.018], P = 0.714).

### White Matter Graph Measures of the Type 2 Diabetes–Based Standard Network

After thresholding all individual networks by use of the prediabetes- or type 2 diabetes–based networks, graph analysis was performed. In Table 2, the associations of these graph measures at a sparsity of 0.8 are shown. In the prediabetes-based standard network, prediabetes was significantly associated with a lower normalized clustering coefficient compared with NGM, which indicates a lower local connectivity. Prediabetes was also associated with a lower normalized average local efficiency. No association was found between prediabetes and the normalized global efficiency and communicability. In addition, type 2 diabetes was associated with higher communicability as compared with NGM, despite the lower node degree. The other three graph measures were not significantly associated with type 2 diabetes. Graph measures for a range of sparsity thresholds are shown in Supplementary Fig. 2. After full adjustment, only the association with higher communicability in type 2 diabetes remained significant. No associations remained significant for prediabetes. A higher communicability was also found for higher continuous glucose measures, and this remained significant after full adjustment (Supplementary Table 4).

Diabetes and Aging

Multiple linear regression analysis was used to determine the relative association of prediabetes and type 2 diabetes with node degree as compared with aging. Node degree was significantly lower in subjects with prediabetes or type 2 diabetes compared with NGM and corresponded to 2.3 or 10.4 years
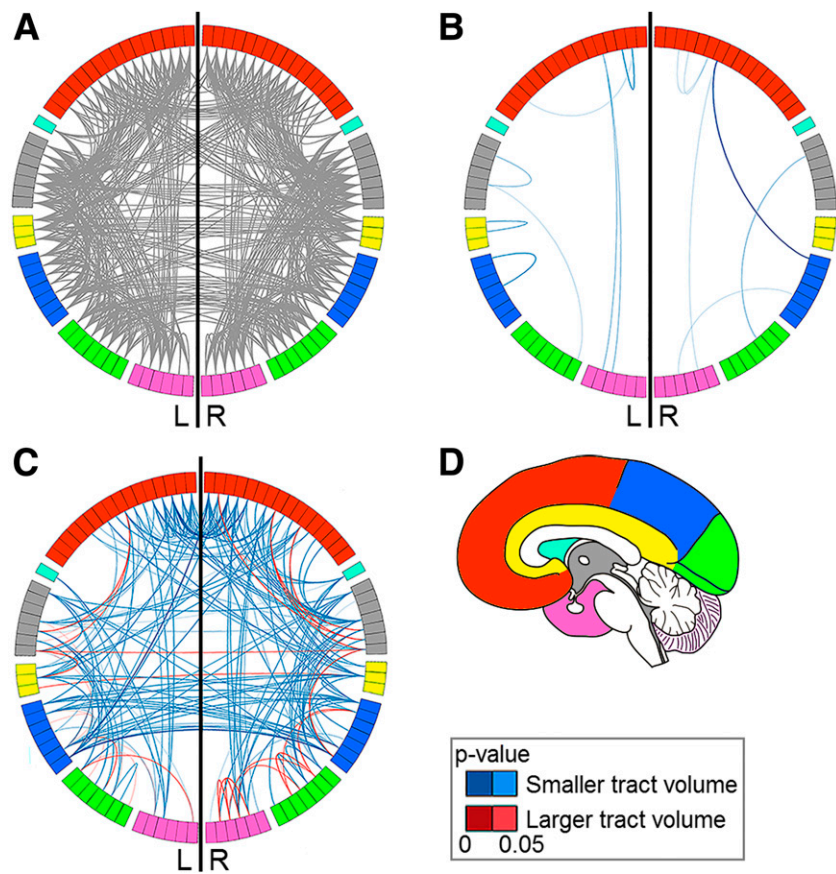
Figure 2—Schematic representation of connections between the atlas regions (for the legend of the regions, see Supplementary Fig. 3) present in the NGM-based standard network (A), and those connections which had a significantly different tract volume in subjects with prediabetes (B) or type 2 diabetes (C) compared with subjects with NGM. Blue connection lines indicate connections with significantly smaller tract volumes (unstandardized β <0) and red lines connections with significantly larger tract volumes (unstandardized β >0). P < 0.05, false discovery rate corrected. Darker blue or red connection lines indicate lower P values. D: Brain regions that represent the color-coded brain regions.

of aging, respectively (Supplementary Table 5). Adjustment for potential confounders (i.e., BMI, systolic blood pressure, ratio of total cholesterol to HDL, prior cardiovascular disease, and antihypertensive and lipid-lowering medication) did not substantially change these results.

There were also connections where tract volumes were significantly associated with age (Supplementary Fig. 3A). Please note the large similarities between connection tract volumes associated with age and type 2 diabetes. However, in type 2 diabetes, the connections between the left and right hippocampus and between right frontal and temporal regions had significantly smaller tract volumes compared with NGM, but these connections were not associated with age (Supplementary Fig. 3B).

CONCLUSIONS

In this study, we found that both prediabetes and type 2 diabetes were associated with a lower node degree, and thus fewer white matter connections, as compared with NGM. Continuous measures of hyperglycemia (HbA$_{1c}$, FBG, and 2-h postload glucose levels) were also associated with lower node degree. Moreover, prediabetes and type 2 diabetes were associated with smaller tract volumes of several connections between cortical regions, which were comparable with those associated with aging. The lower node degree of 0.4 and 1.3% in subjects with prediabetes and type 2 diabetes, respectively, compared with NGM, was equivalent to 2.3 and 10.4 years of aging, which fits with the idea that (pre)diabetes is accompanied by accelerated aging. We also investigated the association between prediabetes and type 2 diabetes and structural organization. In prediabetes compared with NGM, the local efficiency and clustering coefficient were lower,

Table 2—Associations of prediabetes and type 2 diabetes with graph network measures at a sparsity value of 0.8

Normalized graph measures	Prediabetes, stβ (95% CI)*	P	Type 2 diabetes, stβ (95% CI)†	P
Clustering coefficient				
Model 1	**−0.097 (−0.189, −0.005)**	**0.049**	−0.026 (−0.111, 0.059)	0.562
Model 2	−0.066 (−0.161, 0.028)	0.169	0.027 (−0.074, 0.128)	0.603
Global efficiency				
Model 1	0.034 (−0.086, 0.151)	0.625	−0.056 (−0.164, 0.052)	0.212
Model 2	0.032 (−0.092, 0.156)	0.615	−0.051 (−0.180, 0.077)	0.434
Local efficiency				
Model 1	**−0.084 (−0.159, −0.008)**	**0.033**	−0.043 (−0.113, 0.027)	0.208
Model 2	−0.060 (−0.137, 0.017)	0.128	0.010 (−0.073, 0.093)	0.816
Communicability				
Model 1	0.026 (−0.092, 0.144)	0.475	**0.148 (0.042, 0.253)**	**0.008**
Model 2	0.043 (−0.079, 0.165)	0.491	**0.163 (0.037, 0.290)**	**0.011**

Associations of prediabetes and type 2 diabetes with graph measures. Standardized regression coefficients and 95% CI indicate the mean difference in clustering coefficient, global efficiency, local efficiency, and communicability of participants with prediabetes or type 2 diabetes compared with NGM. Model 1 was adjusted for age, sex, education, average node degree, and MRI date. Model 2 was the same as model 1 and additionally adjusted for BMI, office systolic blood pressure, ratio of total cholesterol to HDL, antihypertensive medication, lipid-lowering medication, and history of cardiovascular disease. Boldface type indicates P < 0.05. *Prediabetes-based standard network. †Type 2 diabetes–based standard network.

which indicates that there was a weaker local connectivity. In type 2 diabetes compared with NGM, a higher communicability was found, indicating that in type 2 diabetes, more alternative white matter connections are used to facilitate structural connectivity between brain regions.

In prediabetes, the clustering coefficient and local efficiency were lower compared with NGM, indicating that structural alterations can be observed already in prediabetes. These findings indicate that brain changes already occur in prediabetes before the clinical diagnosis of type 2 diabetes. Therefore, treatment of prediabetes should be considered as a potential target of intervention for the prevention of complications of type 2 diabetes, including structural brain changes. In type 2 diabetes compared with NGM, a higher communicability was found. Communicability is a measure that indicates the ease of communication between two brain regions, taking into account not only the shortest path but also all other possible paths connecting them. A potential explanation for the higher communicability in type 2 diabetes compared with NGM involves the increased WML load in type 2 diabetes and prediabetes (7). The brain might be able to adapt to changing circumstances (to a small extent), and staying physically and mentally fit can possibly promote this effect (34,35). However, the precise pathophysiological basis of white matter alterations in patients with (pre)diabetes remains to be elucidated, and a complex interplay of endocrinological, metabolic, and vascular mechanisms is likely involved (5,7).

Our findings are in line with previous studies that assessed the association between type 2 diabetes and white matter connectivity. Previous reports showed lower white matter connectivity between the hippocampus and the frontal lobe (13), and microstructural abnormalities in four major white matter tracts connecting the frontal, parietal, and temporal lobe (12) in type 2 diabetes compared with a control group. In contrast, a study comparing 55 age-, sex-, and education-matched individuals with type 2 diabetes with 50 individuals without diabetes (11) found that the mean clustering coefficients and global efficiency were lower in subjects with type 2 diabetes compared with control subjects. However, the total number of connections in the network did not differ between the groups, and these between-group differences were independent of vascular lesion load. This difference in observations may be due to the much smaller sample size and the differences in the specific networks, which were analyzed in that study. Interestingly, altered functional connectivity, in terms of a higher clustering coefficient and high local efficiency, was found in type 2 diabetes and at a lower level in prediabetes (36), which was interpreted as a compensatory mechanism in the form of functional reorganization to counteract a decrease in cognitive performance. This is in agreement with the altered structural connectivity observed in the current study, which is indicative of alternative white matter connections in type 2 diabetes.

Study Considerations
The strengths of this study are the sample size and population-based design with an oversampling of participants with type 2 diabetes, which enables an accurate comparison between the three glucose metabolism groups. The large amount of diffusion MRI scans available were semiautomatically processed blinded to group status, which ensures an objective analysis. Other strengths were the use of HbA$_{1c}$ levels and a 2-h OGTT to accurately characterize glucose metabolism and the extensive assessment of potential confounders. In this study, most findings were robust over a large sparsity range and remained statistically significant after adjustment for potential confounders. There are also some limitations. First, the time between baseline measurements and MRI scan might have influenced the associations observed. However, when we additionally adjusted for this, associations did not significantly change. Second, we used a single OGTT to assess (pre)diabetes status, which may result in the misclassification of long-term glucose tolerance status (37). When group sizes and misclassification estimates (37) are taken into account, the net result of this misclassification is likely to be underestimation of brain abnormalities in the group with prediabetes. Furthermore, individuals who underwent MRI were younger, less likely to have type 2 diabetes, less often current smokers, and less often had a low educational level, as compared with the study population that did not undergo MRI. However, as included individuals with MRI data were relatively more healthy compared with those without MRI, our current selection may have caused us to underestimate any of the associations between glucose metabolism status and network measures. And finally, due to the cross-sectional design of the study, we cannot infer any conclusion about the causality of this association. Therefore, future longitudinal studies are needed to address if hyperglycemia preceeds the development of the observed brain abnormalities, which may infer causality.

Conclusion
We showed, in a population-based study, that prediabetes, type 2 diabetes, and continuous measures of hyperglycemia are associated with fewer white matter connections and weaker organization of white matter networks. In addition, type 2 diabetes was associated with higher communicability, which was not yet observed in prediabetes and may reflect the use of alternative white matter connections. These findings support the concept that hyperglycemia, even in the prediabetes phase, may be harmful to the brain, and that type 2 diabetes affects the global and local organization of brain structures.

design or conduct of the study, the preparation of the manuscript, and the decision to submit for publication, and all verify the accuracy and completeness of the data and analyses. L.W.V., M.T.S., W.H.B., and J.F.J. analyzed data and drafted the manuscript. L.W.V., M.T.S., J.J.d.J., C.D.S., N.C.S., R.M.H., C.J.v.d.K., P.C.D., M.P.v.B., S.J.E., W.H.B., and J.F.J. commented on the drafts and contributed to writing. L.W.V., M.T.S., J.J.d.J., C.D.S., N.C.S., R.M.H., C.J.v.d.K., P.C.D., M.P.v.B., S.J.E., W.H.B., and J.F.J. approved the final version of the manuscript. L.W.V. is the guarantor of this work and, as such, had full access to all the data in the study and takes responsibility for the integrity of the data and the accuracy of the data analysis.

References

1. van Bussel FCG, Backes WH, Hofman PAM, et al. Cerebral pathology and cognition in diabetes: the merits of multiparametric neuroimaging. Front Neurosci 2017;11:188
2. Biessels GJ, Reijmer YD. Brain changes underlying cognitive dysfunction in diabetes: what can we learn from MRI? Diabetes 2014;63:2244–2252
3. Geijselaers SLC, Sep SJS, Stehouwer CDA, Biessels GJ. Glucose regulation, cognition, and brain MRI in type 2 diabetes: a systematic review. Lancet Diabetes Endocrinol 2015;3:75–89
4. Awad N, Gagnon M, Messier C. The relationship between impaired glucose tolerance, type 2 diabetes, and cognitive function. J Clin Exp Neuropsychol 2004;26:1044–1080
5. Biessels GJ, Staekenborg S, Brunner E, Brayne C, Scheltens P. Risk of dementia in diabetes mellitus: a systematic review. Lancet Neurol 2006;5:64–74
6. Schneider ALC, Selvin E, Sharrett AR, et al. Diabetes, prediabetes, and brain volumes and subclinical cerebrovascular disease on MRI: the Atherosclerosis Risk in Communities Neurocognitive Study (ARIC-NCS). Diabetes Care 2017;40:1514–1521
7. van Agtmaal MJM, Houben AJHM, de Wit V, et al. Prediabetes is associated with structural brain abnormalities: the Maastricht Study. Diabetes Care 2018;41:2535–2543
8. Marseglia A, Fratiglioni L, Kalpouzos G, Wang R, Bäckman L, Xu W. Prediabetes and diabetes accelerate cognitive decline and predict microvascular lesions: a population-based cohort study. Alzheimers Dement 2019;15:25–33
9. American Diabetes Association. Diagnosis and classification of diabetes mellitus. Diabetes Care 2011;34(Suppl. 1):S62–S69
10. World Health Organization. *Global Report on Diabetes*. Geneva, World Health Organization, 2016

11. Reijmer YD, Leemans A, Brundel M, Kappelle LJ, Biessels GJ; Utrecht Vascular Cognitive Impairment Study Group. Disruption of the cerebral white matter network is related to slowing of information processing speed in patients with type 2 diabetes. Diabetes 2013;62:2112–2115
12. Reijmer YD, Brundel M, de Bresser J, Kappelle LJ, Leemans A, Biessels GJ; Utrecht Vascular Cognitive Impairment Study Group. Microstructural white matter abnormalities and cognitive functioning in type 2 diabetes: a diffusion tensor imaging study. Diabetes Care 2013;36:137–144
13. van Bussel FC, Backes WH, Hofman PA, et al. Altered hippocampal white matter connectivity in type 2 diabetes mellitus and memory decrements. J Neuroendocrinol 2016;28:12366
14. Hsu JL, Chen YL, Leu JG, et al. Microstructural white matter abnormalities in type 2 diabetes mellitus: a diffusion tensor imaging study. Neuroimage 2012;59:1098–1105
15. Watts DJ, Strogatz SH. Collective dynamics of 'small-world' networks. Nature 1998;393:440–442
16. Stam CJ, Reijneveld JC. Graph theoretical analysis of complex networks in the brain. Nonlinear Biomed Phys 2007;1:3
17. Bullmore E, Sporns O. Complex brain networks: graph theoretical analysis of structural and functional systems. Nat Rev Neurosci 2009;10:186–198
18. Schram MT, Sep SJS, van der Kallen CJ, et al. The Maastricht Study: an extensive phenotyping study on determinants of type 2 diabetes, its complications and its comorbidities. Eur J Epidemiol 2014;29:439–451
19. World Health Organization. *Definition and Diagnosis of Diabetes Mellitus and Intermediate Hyperglycemia: Report of a WHO/IDF Consultation*. Geneva, World Health Organization, 2006
20. Tzourio-Mazoyer N, Landeau B, Papathanassiou D, et al. Automated anatomical labeling of activations in SPM using a macroscopic anatomical parcellation of the MNI MRI single-subject brain. Neuroimage 2002;15:273–289
21. Fonov V, Evans AC, Botteron K, Almli CR, McKinstry RC, Collins DL; Brain Development Cooperative Group. Unbiased average age-appropriate atlases for pediatric studies. Neuroimage 2011;54:313–327
22. Vrooman HA, Cocosco CA, van der Lijn F, et al. Multi-spectral brain tissue segmentation using automatically trained k-nearest-neighbor classification. Neuroimage 2007;37:71–81
23. de Boer R, Vrooman HA, van der Lijn F, et al. White matter lesion extension to automatic brain tissue segmentation on MRI. Neuroimage 2009; 45:1151–1161
24. Leemans A, Jeurissen B, Sijbers J, Jones D. ExploreDTI: a graphical toolbox for processing,

analyzing, and visualizing diffusion MR data. In *Proceedings of the 17th Scientific Meeting, International Society for Magnetic Resonance in Medicine, Honolulu, HI, 2009*. p. 3537
25. Tournier JD, Calamante F, Connelly A. Determination of the appropriate b value and number of gradient directions for high-angular-resolution diffusion-weighted imaging. NMR Biomed 2013;26:1775–1786
26. Jeurissen B, Leemans A, Jones DK, Tournier J-D, Sijbers J. Probabilistic fiber tracking using the residual bootstrap with constrained spherical deconvolution. Hum Brain Mapp 2011;32:461–479
27. Vaessen MJ, Jansen JFA, Vlooswijk MCG, et al. White matter network abnormalities are associated with cognitive decline in chronic epilepsy. Cereb Cortex 2012;22:2139–2147
28. Whitwell JL, Crum WR, Watt HC, Fox NC. Normalization of cerebral volumes by use of intracranial volume: implications for longitudinal quantitative MR imaging. AJNR Am J Neuroradiol 2001;22:1483–1489
29. Rubinov M, Sporns O. Complex network measures of brain connectivity: uses and interpretations. Neuroimage 2010;52:1059–1069
30. Latora V, Marchiori M. Efficient behavior of small-world networks. Phys Rev Lett 2001;87:198701
31. Estrada E, Hatano N, Benzi M. The physics of communicability in complex networks. Phys Rep 2012;514:89–119
32. de Reus MA, van den Heuvel MP. Estimating false positives and negatives in brain networks. Neuroimage 2013;70:402–409
33. van den Heuvel MP, Sporns O. Rich-club organization of the human connectome. J Neurosci 2011;31:15775–15786
34. Sexton CE, Betts JF, Demnitz N, Dawes H, Ebmeier KP, Johansen-Berg H. A systematic review of MRI studies examining the relationship between physical fitness and activity and the white matter of the ageing brain. Neuroimage 2016;131:81–90
35. Phillips C. Lifestyle modulators of neuroplasticity: how physical activity, mental engagement, and diet promote cognitive health during aging. Neural Plast 2017;2017:3589271–3589271
36. van Bussel FC, Backes WH, van Veenendaal TM, et al. Functional brain networks are altered in type 2 diabetes and prediabetes: signs for compensation of cognitive decrements? The Maastricht Study. Diabetes 2016;65:2404–2413
37. Mooy JM, Grootenhuis PA, de Vries H, et al. Intra-individual variation of glucose, specific insulin and proinsulin concentrations measured by two oral glucose tolerance tests in a general Caucasian population: the Hoorn Study. Diabetologia 1996;39:298–305